Carpathian Journal of Earth and Environmental Sciences, August 2018, Vol. 13, No. 2, p. 395 - 408; DOI:10.26471/cjees/2018/013/034

SPATIO-TEMPORAL ANALYSIS OF SURFACE URBAN HEAT ISLAND BASED ON LANDSAT ETM+ AND OLI/TIRS IMAGERY IN THE CITY OF KOŠICE, SLOVAKIA

Katarína ONAČILLOVÁ[1*] & Michal GALLAY[1]

[1]Institute of Geography, Faculty of Science, Pavol Jozef Šafárik University in Košice, Jesenná 5, 040 01 Košice, Slovakia, e-mail: onacillova.katarina@gmail.com

Abstract: The availability of multispectral imagery including a thermal infrared band enabled monitoring the spatial pattern of land surface temperature (LST) and linking it with land cover properties. Multispectral data archives allow for assessing the dynamics of urban heat island (UHI) by the means of LST mapping for particular area. The research on UHI has been focused on large cities where the phenomenon is the most pronounced. However, UHI concerns also smaller cities which are more abundant and over a half of urban population lives in cities with less than a half of million inhabitants. Therefore, this paper focuses on assessing the pattern of the UHI in the city of Košice as an example of a typical small post-communist Central European city after changes of urban landscape induced by transition to capitalism and modern trends in economy. We demonstrate the effect of urban greenery on the UHI phenomenon in Košice using the Landsat 7 and Landsat 8 imagery and ground-based weather station data. We determine differences in the LST distribution in the city under various weather conditions in the vegetation season from 2013 to 2015. The results revealed the spatial pattern of the LST and UHI in Košice which is unique from regional perspective. Globally, the results support the hypotesis that UHI poses problem even in such a small city. Expansion of urban fabric by construction of new residential, commercial and industrial estates and also building new traffic infrastructure in last few years amplified the UHI. Strong correlation was calculated between the LST and the amount of urban greenery in the city. Even narrow green alleys or small parks are capable of mitigating the UHI phenomenon which can be a usefull argument for officials in Košice but also in other cities to support investments in development of green areas.

Keywords: urban heat island, Košice city, Landsat, land surface temperature, land cover

1. INTRODUCTION

The tendency of world population to live in towns and cities is exponentially growing. Today, nearly 4 billion of people live in urban areas (UN, 2014) often experiencing overheating of their environment. Urbanization and low energy consumption for vapour that is transformed into heat energy causes significant differences in temperatures between overheated areas of cities and less affected countryside where the percentage of vegetation is higher. It leads to the phenomenon of urban heat island (UHI) defined by Oke (1973) as an industrialized area of the city (sometimes also the city itself) that differs from the surrounding rural area by higher temperature – a result of the impact of human activities and increasing rate of urbanization. Also it tends to be stronger on weekdays compared to the weekend, due to increased anthropogenic activity (Kim & Baik, 2004). There is also a close correlation between the magnitude of UHI and weather conditions – relative humidity, cloud cover, precipitation or wind speed. UHI is most pronounced during warm, clear and windless days which was found e.g. by Giannaros et al., (2010) in Thessaloniki, Greece. The UHI is generally more effective in the night time (Voogt & Oke, 2003) when the urban areas reradiate the heat accumulated during the daytime while the air and surface temperatures are lower in the surrounding rural areas what was demonstrated by Gerçek et al., (2016) in Izmit, Turkey. The effect of UHI is determined also by geographical properties such as the extent of the city, urban morphology, regional climate, slope and aspect of terrain, altitude,

spatial structure and composition of land cover. The impact of the UHI includes rising energy and water consumption, more intense heat waves during the summer, and higher risks of heat-related morbidity and mortality, particularly for young children, elderly people, and low-income urban residents (Výberči et al., 2017).

The classical indicator to describe a surface urban heat island is the difference between urban and rural surface temperatures. With the advent of thermal remote sensing from spaceborne platforms the UHI has been evaluated by the means of land surface temperature (LST). The LST is defined as the temperature of the interface between the Earth's surface and its atmosphere. On the other hand, the air temperature (T-air) is measured at 1.5 to 2 m by meteorological weather stations which can significantly underestimate the actual radiative surface temperature, especially at high temperatures and in non-forested areas. For this reason, many recent studies operate with LST rather than T-air to describe the spatial variation of temperature in urban environment. The UHI analysed on the basis of LST is specifically termed the surface UHI (Voogt & Oke, 2003). LST has advantage of spatially explicit datasets, compared to single air temperature measurement at points or traverses through the urban landscape.

Spatial and temporal resolutions of thermal satellite sensors differ which determines the main applications of the data. The MODIS sensor, on-board the Terra and Aqua satellites, or the Advanced Very High Resolution Radiometer (AVHRR) are example of sensors which main benefit is in the short revisit period of 24 hours thus providing high resolution in the time domain of the LST dynamics. However, the spatial resolution of the acquired thermal data is rather coarse (250 m for MODIS, 1000 m for AVHRR) which is suitable for global to regional scale studies (e.g. Cheval et al., 2011, Schwartz et al., 2011, Stathopoulou et al., 2004).

On the other hand, there is The Landsat Thematic Mapper (TM), Enhanced Thematic Mapper Plus (ETM+), Operational Land Imager/Thermal Infrared Sensor (OLI/TIRS) and Advanced Spaceborne Thermal Emission and Reflection Radiometer (ASTER) thermal imagery all have a moderate spatial resolution of 60 m or 100 m. The Landsat series of the Earth observation satellites provide the most commonly used data for LST mapping (TM, ETM+, OLI/TIRS). The Landsat program is managed by The National Aeronautics and Space Administration (NASA) and The United States Geological Survey (USGS) of the United States (Wulder et al., 2016; Loveland & Irons, 2016). The Landsat 5 TM is not operational, but the data archive is available freely. LST for the last two decades has been recorded by the Landsat 7 and Landsat 8 satellites (NASA, 2013). Both satellites orbit and provide seasonal coverage of the global landmass with a 16-day repeat cycle (except for the highest polar latitudes) in an 8-day offset from each other. Although the revisit frequency is longer than for the MODIS sensor, the spatial resolution of acquired imagery is higher. The Landsat 7 satellite is in operation since 1999. It carries the Enhanced Thematic Mapper Plus (ETM+) passive sensor mapping the earth surface in eight spectral bands with a spatial resolution of 30 meters for Bands 1-7 (thermal band is resampled to 30-meter pixel) and 15 meters for Band 8 (panchromatic). However, on May 31, 2003 the Scan Line Corrector (SLC) in the ETM+ instrument failed, what causes that the satellite images have a "zig-zag" pattern, resulting in some areas that are imaged twice and others that are not imaged at all. Despite this technical complication, Landsat 7 serves as an important tool for assessing the impact of urbanization on UHI in big cities (Rajasekar & Weng, 2009, Chen et al., 2015). The Landsat 8 was launched on February 11, 2013 and its payload consists of two remote sensing instruments - the Operational Land Imager (OLI) and the Thermal Infrared Sensor (TIRS) with a spatial resolution of 30 meters for visible, near infrared and short-wavelength infrared bands, 15 meters for panchromatic Band 8 and 100 meters for thermal Bands 10 and 11 (that are resampled to 30-meter pixels). To date, both ETM+ and OLI/TIRS sensors provide the highest spatial resolution for monitoring the LST from space.

A plethora of studies explored this benefit, however, focusing mainly on big world cities. Large cities such as Bucharest (Cheval & Dumitrescu, 2009), Rome (Fabrizi et al., 2010), Budapest (Pongrácz et al., 2010), Buenos Aires (Camilloni & Barrucand, 2011), Rotterdam (Klok et al., 2012), Moscow (Lokoshchenko, 2014), Beijing (Chen et al., 2015), Manchester (Levermore et al., 2017) have been studied in this context. The officials of such cities started to realize urgency of the current situation connected with urbanization and try to make first steps towards easing UHI effect, because increasing temperatures of UHI are a sign of increasing air pollution, global warming, affecting comfort of urban citizens and leading even to greater health risks. But UHI also concerns smaller cities inhabited by several tens to hundred thousands of inhabitants which are numerous and many are growing rapidly (UN, 2014). Such cities are typical, for example, in the central eastern European area and have not been under the main scope of UHI studies,

although exceptions exist. The spatial distribution of UHI for smaller cities has been investigated for small-sized cities such as Szeged (Mucsi et al., 2014) and medium-sized cities such as Brno (Dobrovolný, 2013), Poznań (Majkowska et al., 2016) or Bratislava (Rusňák & Lieskovský, 2017). Overall, almost half of the world's urban dwellers reside in settlements with fewer than half a million inhabitants, while only around 12% live in the 28 mega-cities with more than 10 million inhabitants (UN, 2014).

Although, it is known to exist and cause problems in small cities during summer season, there is lack of published studies elucidating spatial and temporal aspects of the UHI pehnomenon. Such research can provide arguments for decision makers, urban planners and managers that UHI concerns also their cities and can be mitigated by investments into local land cover change. Therefore, this paper focuses on the UHI phenomenon in Košice in Eastern Slovakia, as an example of a small city housing over 239 thousand people. The city underwent transformation of urban space typical for a post-communist city, which is similar to many other cities in Central Europe. The main aim is to analyse the spatial distribution of LST and its seasonal change throughout year in relation to land cover. UHI is known to exist in Košice, but it has not been yet quantified with modern geospatial approaches explointing the benefits of multispectral satellite data. This study provides a broader scale view on the local climate in Košice linking to the results of Hofierka et al., (2017) who investigated high-resolution monitoring of vegetation for modelling the cooling effect of urban greenery in Košice.

2. STUDY AREA

The area of interest comprises the administrative region of the Košice City situated in Eastern Slovakia, Central Europe (Fig. 1). It is the second largest city in Slovakia with 239 200 inhabitants in 2017 (Statistical Office, 2016). The written records of establishing the city date back to 13th century A.D, but the area was inhabited since prehistorical times. Košice had been expanding in the valley of the Hornád River and its terraces at the foothill of Volovské vrchy and Čierna hora Mountains. Total area of the city is 243.75 km^2 and the altitudes range from 184 m a.s.l. to 851 m a.s.l. The city centre lies at 208 m a.s.l.

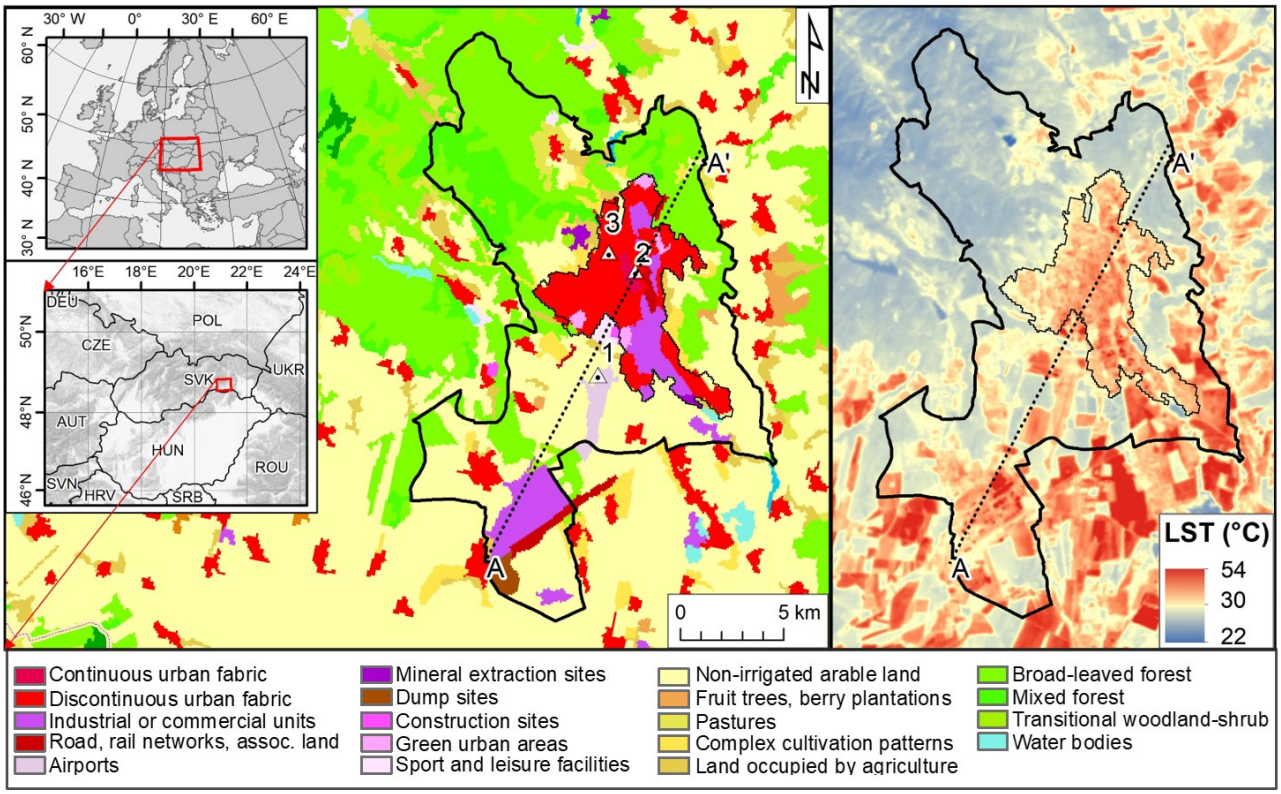

Figure 1. Location of the Košice City as the administrative area (thick black solid line) and urbanized core (thin black solid line) overlaid on CORINE Land Cover 2012 and land surface temperature (LST) 6 August 2015 with the meteorological stations at the airport (1), city centre (2), and at the Technical University in Košice (3). Vertical profile along the line A-A‘ is displayed in Figure 3.

The climate is moderate in the transition zone between humid continental and oceanic climate (Climate Atlas of Slovakia, 2014). Mean annual temperatures range between 8 - 9 °C reaching maximum of the mean monthly temperature in July (19.5 °C) and minimum in January (-3 °C). The occurrence of hot summer periods when air temperature rises above 35 °C is becoming more frequent since the last two decades. Such days are mostly concentrated in July and beginning of August (Švec et al., 2016).

According to the CORINE Land Cover (CLC) 2012 (Copernicus Land Monitoring Service, 2016) continuous and discontinuous urban fabric including roads, railways and other impervious surface categories cover over 57 km^2 which is nearly 24 % of the area. Forests extend over 32 % of the area in the north and east of the city but green urban areas open to the public that include urban parks and gardens, fringes of transport corridors and street trees and verges cover only 0.62 %.

3. DATA AND METHODS

The research in this study takes advantage of multispectral satellite imagery and meteorological observations. The multispectral scenes of Landsat 8 OLI/TIRS (5 scenes) and Landsat 7 ETM+ (7 scenes) were downloaded using USGS EarthExplorer web service (https://earthexplorer.usgs.gov).

The imagery was selected to cover the vegetation season (from early spring to late autumn) with the lowest cloud cover possible for three consecutive years of 2013-2015. The winter season was not considered as the available imagery due to the fact that it was not completely clear from clouds for the studied area for the observed period. For this reason, it was not possible to compile suitable time series. Also, the UHI phenomenon, though occurring in cold months, has not such a dangerous influence on human activities and vegetation or animals as opposed to the summer season.

The multispectral imagery was processed using a pipeline shown in figure 2 to derive brightness land surface temperature (LST) per pixel of the thermal band records. A review of the principles and method is described in Li et al., (2013). In short, the approach can be split into three main steps. The ETM+ sensor and the TIRS sensor record the brightness at the top of the atmosphere (TOA) and store the information in the form of digital numbers (DN) in the range 0-255 (8 bits) for Landsat 7 and 0-65,536 (16 bits) for Landsat 8, respectively. As the ETM+ data contain wedge-shaped gaps on both sides of each scene due to the failure of the scan line corrector (SLC-off) in 2003, the

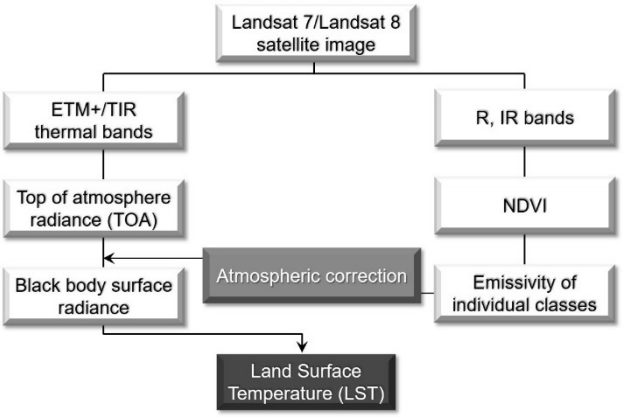

Figure 2. Flowchart summarizing basic steps of LST derivation from imagery

missing DN values in Landsat 7 scenes were interpolated using the inverse distance weighting method implemented in the Analyses, Fill No Data tool, of the QGIS software (www.qgis.org). In the first step of processing, the DN values were converted to spectral radiances using values of the gain and bias contained in the metadata using the USGS formulas:

$$L_{TOA} = M_L Q_{CAL} + A_L \quad (1)$$

where L_{TOA} is TOA spectral radiance in W.m^{-2}.srad^{-1}.μm^{-1}, M_L is a band-specific multiplicative rescaling factor from the metadata, A_L is a band-specific additive rescaling factor from the metadata, Q_{cal} is quantized and calibrated standard product pixel values (DN). The Band 10 of OLI/TIRS sensor and Band 7 of ETM+ sensor was used for calculating L_{TOA}.

Then, the L_{TOA} was transferred to surface leaving radiance by removing atmospheric effects, employing the land surface emissivity method using NDVI proposed in Zhang et al., (2006) to calculate the emissivity (ε) of a real surface (Table 1) and the Atmospheric Correction Parameter Calculator developed by Barsi et al., (2005) that uses the MODTRAN radiative transfer model to calculate the three parameters that are necessary for atmospheric correction: upwelling radiance (L_u), downwelling radiance (L_d), and transmission coefficient (τ) (Table 2).

Table 1. Reclassification of NDVI raster values to land surface emissivity (ε) after Zhang et al., (2006)

NDVI	ε
NDVI < - 0.185	0.995
-0.185 ≤ NDVI < 0.157	0.985
0.157 ≤ NDVI ≤ 0.727	1.009 + 0.047*ln(NDVI)
NDVI > 0.727	0.990

Table 2. Parameters used for atmospheric correction of the Landsat imagery after Barsi et al., (2005).

Senzor type	Date of acquisition	Atmospheric transmittance	Upwelling Radiance ($W.m^{-2}.srad^{-1}.\mu m^{-1}$)	Downwelling Radiance ($W.m^{-2}.srad^{-1}.\mu m^{-1}$)
L7 ETM+	17 Mar 2013	0.97	0.15	0.25
L7 ETM+	20 May 2013	0.82	1.25	2.06
L8 TIRS	9 Aug 2013	0.78	1.79	2.98
L7 ETM+	28 Nov 2013	0.90	0.53	0.89
L8 TIRS	12 Mar 2014	0.94	0.35	0.60
L7 ETM+	7 May 2014	0.85	0.94	1.57
L7 ETM+	11 Aug 2014	0.62	2.79	4.34
L7 ETM+	15 Nov 2014	0.87	0.80	1.36
L8 TIRS	8 Mar 2015	0.92	0.47	0.80
L8 TIRS	18 May 2015	0.91	0.58	1.00
L8 TIRS	6 Aug 2015	0.74	2.15	3.49
L7 ETM+	2 Nov 2015	0.95	0.29	0.51

The radiance of a black body surface with kinetic temperature T (L_T) can be expressed as:

$$L_T = \frac{L_{TOA} - L_u - \tau(1-\varepsilon)L_d}{\tau\varepsilon} \quad (2)$$

According to Barsi et al., (2005), uncertainties in LST related to the below method of atmospheric correction should be less than 2 degrees of Kelvin. Land surface emissivity ε raster values were calculated according to Zhang et al., (2006) by reclassifying the normalized difference vegetation index (NDVI) raster values using Table 1. NDVI was calculated in the following way:

$$NDVI = \frac{NIR - RED}{NIR + RED} \quad (3)$$

where *NIR* represents spectral reflectance in near-infrared (Band 4 for Landsat 7, Band 5 for Landsat 8), while *RED* stands for spectral reflectance in the visible red part of the electromagnetic spectrum (Band 3 for Landsat 7, Band 4 for Landsat 8). Then, L_T radiances were recalculated to land surface temperatures *LST* in Kelvins using USGS formulas:

$$LST = \frac{K_2}{ln(\frac{K_1}{L_T} + 1)} \quad (4)$$

where L_T is the surface radiance in Watts/(m^2*srad*μm), K_1 and K_2 are the band-specific thermal conversion constants from the metadata. In the last step, LST (K) was converted into LST (°C):

$$LST\ (C) = LST\ (K) - 273.15 \quad (5)$$

Data from meteorological observation were used to compare the LST values with the air temperatures at the time of image acquisition. Measurements from the station at the airport (Košice - letisko) and in the city centre (Košice - Štefánikova) were provided by the Slovak Hydrometeorological Institute (SHMÚ). Furthermore, we used observation data measured by the weather station of the Department of Cybernetics and Artificial Intelligence, Technical University in Košice. This automated station is located on the roof of a building at the Boženy Němcovej Street, Nr. 3 (Fig. 1).

Land cover types were evaluated using the CLC 2012 geodatabase which spatial scale is comparable with cell size of the source Landsat scenes and derived LST surfaces. Selected land cover types were used to calculate the mean, minimum and maximum values of LST using the Spatial Analyst Tools toolbox and function Zonal Statistics.

There are various indicators of UHI existence (Schwarz et al., 2011). We used two such indicators to evaluate the significance of the differences between mean LST values calculated for urban and rural area. In the first approach, the urban area of Košice was defined as the administrative area (Fig. 1, thick solid black line, 242 km^2) and the rural area as a buffer zone of 10 km outside this area (1,736 km^2). A one-way analysis of variance (ANOVA) of the LST mean values in urban and rural areas was performed.

4. RESULTS

Application of the described methods resulted in a series of geolocated raster data layers and statistics which are reported in the following subsections. Firstly, we focus on the spatial pattern of LST in Košice linking it with the CLC types valid to the year of 2012. Secondly, we report the relation of LST and weather parameters. The third group of results shows how spatial pattern and univariate statistics of LST varied during vegetation season.

4.1. Spatial variability of LST and land cover type

The spatial pattern of LST in the Košice city is very well depicted on the datasets derived from the Landsat 8 scene acquired on August 6, 2015. The presence of the UHI phenomenon in the city is clearly indicated by that the central part of the city and other areas of continuous and discontinuous urban fabric are overheated in comparison with forests, shrubland and pastures (Fig. 1).

Statistical evidence of UHI in Košice for this Landsat 8 scene is provided by the results of the one-way analysis of variance (ANOVA) of LST mean values calculated for urban area and rural area. In the first approach, the mean values and standard deviations of LST (urban: 27.38 °C; 3.34 °C; rural: 26.26 °C; 3.23 °C) were significantly different with p below 0.001. In the second approach, the mean values and standard deviations of LST (urban: 30.05 °C; 1.80 °C; rural: 26.95 °C; 3.28 °C) were also significantly different with p below 0.001. Despite there are large areas of high LST values in the rural zones, the ANOVA tests showed the urban core is statistically hotter than its surroundings.

The highest LST values are clearly co-located with impervious surfaces of urban fabric with lack of vegetation or water surfaces. LST values climbing up to to 50 °C are visible in the industrial zone of the steel works U.S. Steel Košice (southwest area) with abundant metallic roofs and sources of heat.

Still high, but slightly lower LST, occurred in the historical core of the city, areas of recently built shopping centres in the south of the city core, then in the airport area and in areas of urban fabric on the outskirts of the city. It should be noted, that also non-irrigated arable or dump sites radiated large amount of heat which is apparent in the southeast and southwest part of the area. In general, it can be explained by the bare ground surface lacking green vegetation at the time of sensing. On contrary, the lowest LST values form contiguous area related to the Košice forest park in the north-western and north-eastern part of the city, with a high proportion of forest vegetation and low human intervention to the nature. Low temperature values are distributed also along the Hornád river valley.

To characterize the spatial extent of the UHI in Košice city in detail, the profile graph through LST and CLC 2012 pattern was made for the image acquired on August 6, 2015 (Fig. 3). The LST values vary depending on the type of land cover. The LST profile A–A' crosses Košice from southwest to northeast. The mean LST for the profile is 36.8 °C, with a maximum of 50.9 °C and a minimum of 29.1 °C. The line crosses 757 cells of the LST raster layer (22.7 km), and it begins in the main industrial zone of Košice comprising the steel works of the U.S. Steel company, where the LST values are very high, reaching up to 50 °C.

The following two local LST minima demonstrate how even small patches of shrubland can reduce the LST. The two troughs are separated by a local LST peak associated with arable land likely without vegetation cover in that time. Afterwards, LST values rise along with the area of the airport and then the line drops when crossing non-irrigated arable land and land occupied by agriculture. Further on, LST increases sharply over 40 °C which is connected with a large shopping centre, city-centre, road network and industrial area. Clearly visible drops of LST values recorded occur when the line crosses areas of urban greenery before heading to north-eastern borders of Košice formed by forest, where values sharply decrease stabilizing about 30 °C. Local maxima up to 40 °C before entering the forest land occur above the main railway station and motorways separated by the river of Hornád.

The land cover of the Košice study area comprises 19 different types according to the CLC 2012 database. Table 3 reports a statistical summary of LST in selected land cover types. The highest mean LST are related with build-up urban or industrial areas such as continuous urban fabric, industrial or commercial units, dump sites, and discontinuous urban fabric where the average temperatures ranged between 38 to almost 41 °C. On the other hand, low average LST values between almost 27.8 °C to 29.4°C related to the classes of forested land and water bodies. Mean LST of 32°C and 35 °C was recorded within agricultural land and areas of urban greenery and urban areas with green vegetation. Differences of more than 10 °C within the single day are apparent between LST over vegetated areas and areas of water bodies on one hand compared to urban fabric areas and industrial zones with a minimal percentage of green vegetation on the other hand.

4.2 LST variability related to weather characteristics and NDVI

The derived LST raster data were analysed with regard to selected weather characteristics related to the properties of atmosphere near the ground. Relative air humidity and cloud cover were measured at three stations in the city. Table 4 reports the meteorological records and the co-located LST values from the Landsat scene at the particular time of the Landsat scene acquisition.

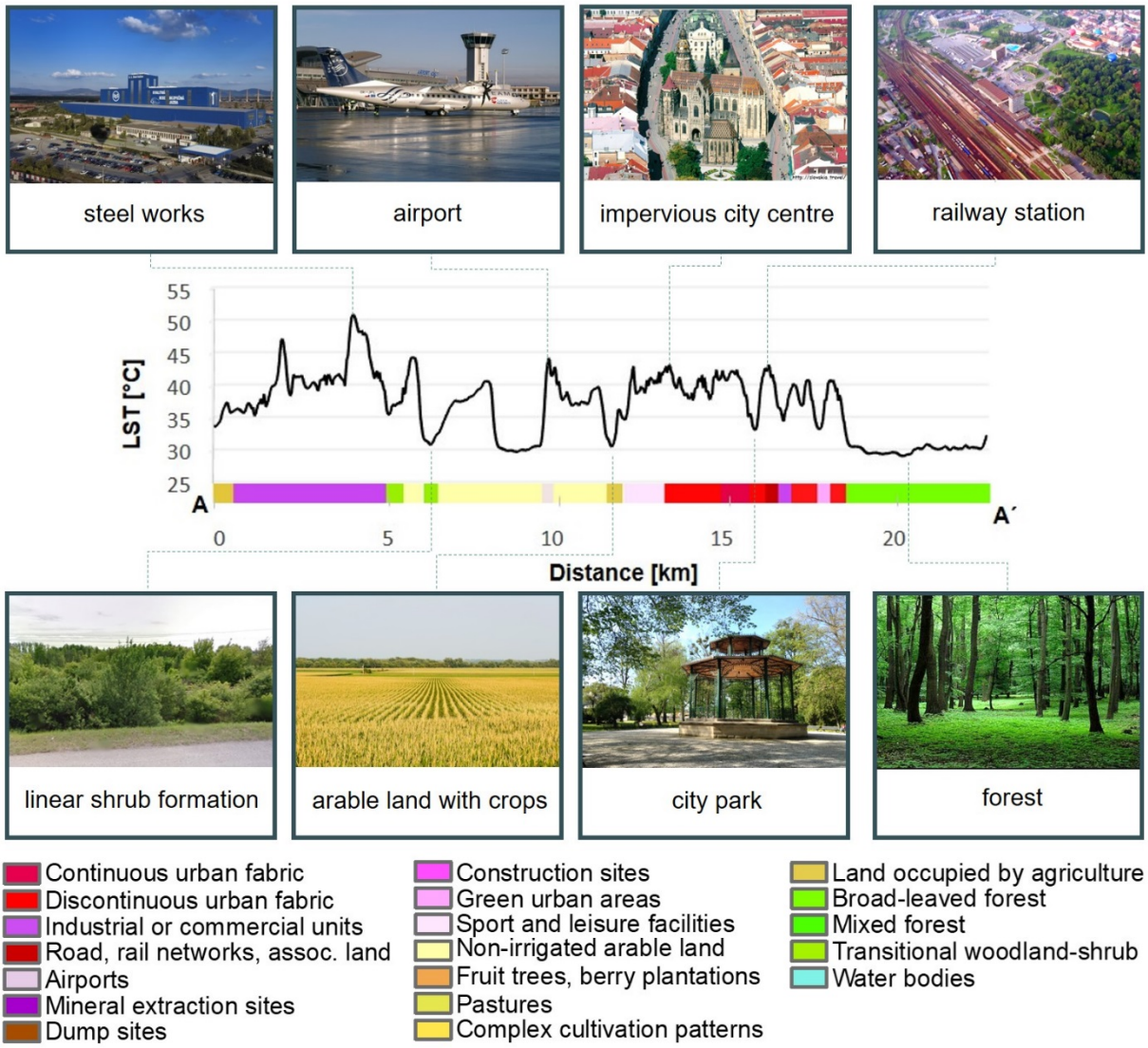

Figure 3. A-A´ profile in Fig. 3 through CLC 2012 land cover classes and the LST surface on 6 August 2015 with photographs illustrating the land cover.

Figure 4 graphically depicts the relationship between LST and meteorological variables. In general, differences between LST values at the weather stations increase with decreasing relative humidity and cloudiness. For instance, during the day with high relative humidity (> 72%) and cloud cover (48%) on November 28, 2011, in selected three locations difference in LST was only about 1 °C (Table 4). The opposite situation occurred on 6 August 2015, when during the day with low relative humidity (< 40%) and very low cloudiness (about 1.16%) differences of LST at the three weather stations exceeded 7 °C. Figure 4 shows the ordinary least squares linear regression models between LST and air temperature and also LST and relative air humidity recorded at the three weather stations from Tab. 4. The regression parameters are significant at p = 0.001. LST and air temperature are strongly positively correlated as indicated also by the Pearson's correlation coefficient (r = 0.966). Coefficient of determination R^2 implies that 93.1% of the variability in air temperature can be explained by the variability in LST (Fig. 4a). Moderate negative correlation (r = -0.526, R^2 = 0.277) was calculated between LST and relative air humidity (Fig. 4b) suggesting that areas of higher relative humidity of air, such as vegetated areas or water surfaces, could contribute to about 28% reduction of land surface temperature. LST and cloudiness were very weakly positively correlated (r = 0.341).

The following analysis was focused on the relationship between the LST and the amount of the vegetation cover per area unit for which the NDVI was used as a proxy parameter. High values of NDVI indicate high reflectance of near-infrared and low reflectance of red portion of spectrum from the land surface which is typical for green vegetation with high chlorophyll content (Fig. 5).

Visual inspection and comparison of Figure 5a and 5b indicates that high NDVI values are co-located with low LST values during the hot summer day of 6 August 2015. The relatively strong negative correlation between NDVI and LST is observed during the vegetation season under the leaf-on conditions which is demonstrated by the graphs in figure 5. The Pearson's r in spring and summer months reached 0.80 and 0.83, respectively.

There is very weak correlation (r = 0.38) observed for late autumn with leaf-off conditions. The graphs depict the situation in selected days, but they convey the general conclusion that UHI phenomenon in the city of Košice can be mitigated by vegetation.

Table 3. Mean, minimum, maximum of LST for selected classes of CORINE Land Cover 2012 on August 6, 2015.

Land cover	Area [%]	Area [ha]	LST (°C)		
			Mean	Min	Max
Continuous urban fabric	0.44	107.65	40.7	36.7	43.2
Industrial or commercial units	7.78	1897.38	40.2	32.1	53.7
Dump sites	0.79	192.54	39.7	31.9	46.4
Discontinuous urban fabric	13.43	3274.48	38.1	27.7	47.2
Green urban areas	0.62	150.97	35.0	29.9	40.3
Land principally occupied by agriculture	1.21	294.06	33.2	26.3	44.1
Broad-leaved forest	26.58	6479.81	29.4	24.8	40.5
Water bodies	0.22	54.26	29.0	27.2	34.0
Mixed forest	6.37	1552.56	27.8	25.6	35.0

Table 4. Parameters of input images, satellite-derived LST and WS air-temperature (T-air).

Satellite image parameters			WS Košice - city			WS Košice - airport			WS Boženy Němcovej 3		
Acquis. date, (satellite)	Scene center time (UTC)	Cloud cover [%]	T-air [°C]	LST [°C]	Relative hum.[%]	T-air [°C]	LST [°C]	Relative hum.[%]	T-air [°C]	LST [°C]	Relative hum.[%]
17.03.2013 (L7)	9:22:47	5.00	-4.4	3.7	63	0.2	4.3	44	0.9	3.6	48
20.05.2013 (L7)	9:22:31	25.00	20.4	27.2	58	22.0	24.4	56	21.4	29.3	63
09.08.2013 (L8)	9:22:29	0.05	30.2	38.4	44	34.9	37.2	24	33.5	40.2	35
28.11.2013 (L7)	9:22:57	48.00	-2.7	0.6	77	0.1	-0.8	72	-0.9	-0.1	72
12.03.2014 (L8)	9:27:12	0.23	9.0	13.8	50	10.8	15.0	37	11.2	15.2	41
07.05.2014 (L7)	9:23:53	27.00	16.2	19.0	54	19.3	18.6	46	18.4	18.6	49
11.08.2014 (L7)	9:24:19	28.00	24.9	30.1	67	27.9	27.1	60	28.8	35.6	57
15.11.2014 (L7)	9:24:55	47.00	10.4	17.5	81	13.5	16.8	67	12.9	18.2	75
08.03.2015 (L8)	9:20:10	1.23	-	11.4	-	6.9	11.2	59	9.3	12.0	54
18.05.2015 (L8)	9:25:41	1.17	-	21.0	-	18.5	28.7	36	18.4	23.9	43
06.08.2015 (L8)	9:20:11	1.16	-	35.8	-	30.5	30.0	36	30.5	37.6	41
02.11.2015 (L7)	9:27:07	30.00	-	3.7	-	7.6	5.5	71	8.0	5.5	75

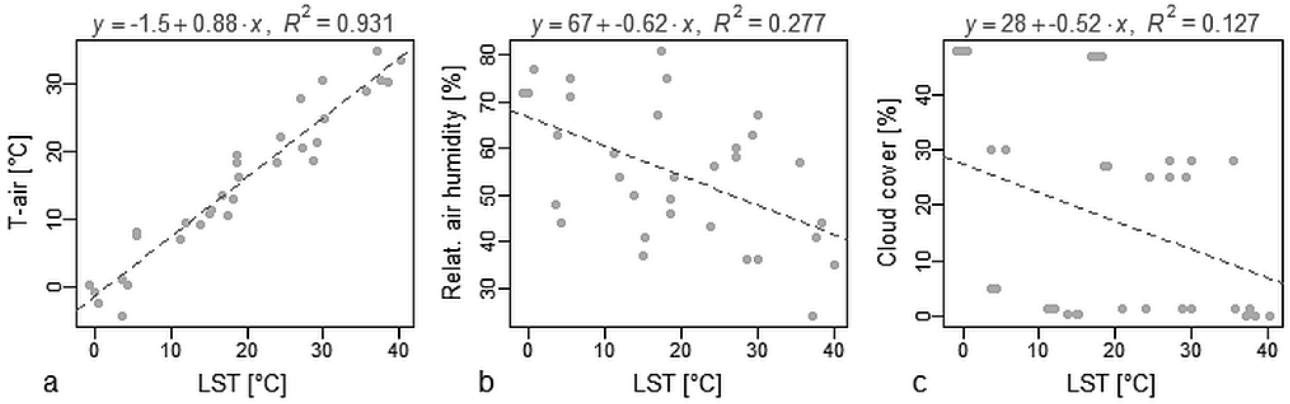

Figure 4. Relationship between LST and (a) air temperature (T-air), (b) relative air humidity, (c) cloud cover on the three weather stations within Košice city with OLS linar regression models (equation and dashed line). Data are reported in Table 4.

This effect is well conveyed by figure 6 which focuses on three areas (1, 2, 3) within the city centre (Fig. 6a). The false colour composite orthophoto, LST and NDVI of Fig. 6b are calculated for 6 August 2015. The surface of land cover in historical core of the city centre (Fig. 6c) is red, meaning high surface temperatures above 40°C. The surroundings of the St. Elisabeth Cathedral are slightly cooler (area 2) likely for the green parks in the vicinity well depicted in Fig. 6d by the higher NDVI values. The vegetation reduces the LST along the Moyzesova Street (area 1) where a tree alley is planted. The LST on the street is 3°C lower than on the adjacent buildings and streets of the historical core with absent vegetation. Large area of urban greenery such as the city park (area 3 in Fig. 6d) relates to the lowest LST (Fig. 6c). It can be inferred from Fig. 6b, 6c and 6d that presence of vegetation even in small extent can effectively reduce temperature within Košice.

4.3. Temporal variability of LST

The time-series of Landsat 7 and Landsat 8 scenes enabled evaluating seasonal change of local variation of LST within the city. Figure 7 shows maps of LST standard deviations calculated in a moving window of 7x7 cells for selected months for three years of 2013, 2014, and 2015.

It is clear that locally the LST differences are relatively low in March and November (early spring and late autumn) when the vegetation has not such an effect on mitigating the UHI phenomenon (dormant season). However, the local LST deviations increased in May and August (the growing season) when the accumulation and re-radiation of heat is strongly differentiated by land cover type. The effect of adjacent areas of low LST on vegetation cover and high LST on urban fabric or industrial areas appears to be the strongest during the summer (highest deviations depicted by red tones).

The temporal aspect of LST can be also demonstrated by the land cover change, for example because of construction. We identified two areas shown in Fig. 8 where grassland was replaced by shopping centre (area 1) and industrial park (area 2) respectively. The current state is displayed in Fig. 8a, the spatial pattern of LST in 2000 is shown in Fig. 8b and the state in 2015 is depicted by Fig. 8c. The most marked differences in the LST were observed in the area of constructed shopping centres south of the city core (Moldavská Street), where the maximum LST was 10°C greater in 2015 than in 2000 before the construction replaced grassland. The mean LST in this area was 35.2°C in 2000 and 38.5°C in 2015. Similarly, the area near the international airport experienced substantial change, where grassland and arable land in 2000 changed into industrial park by 2015. The maximum LST in 2000 in this area reached 43.7°C and the mean value was 37.3°C. After the industrial park was built and in operation in 2015, the maximum LST was about 51.2°C and mean LST about 41.6°C.

Although, the weather conditions on the two dates of sensing the area by Landsat 7 and 8 were not identical the days are comparable as being hot clear sky summer days. This example indicates that such land cover change of the last years, magnifies the UHI effect expanding it also into suburban zones.

5. DISCUSSION

The generated results support findings of other studies achieved in the assessment of LST in big cities or similar cities such as Košice. The analysis of LST derived from selected satellite scenes provided evidence that the UHI phenomenon concerns also the city of Košice which is rather a small city.

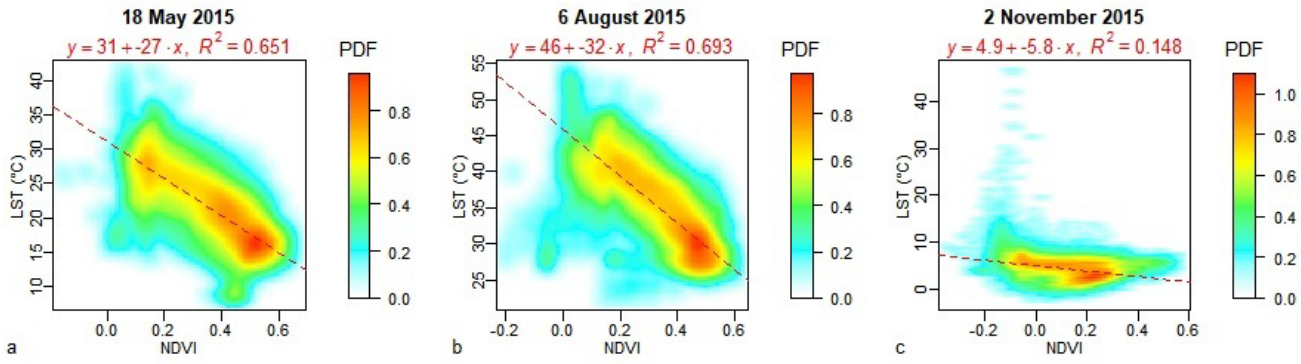

Figure 5. Smoothed scatterplots of LST and NDVI in the administration area of Košice for three selected dates in spring, summer and late autumn. For high density of points in the scatterplots, the points are expressed as the values of probability density function (PDF) resulting from a two-dimensional kernel density estimation. Each scatterplot comprises a linear regression model.

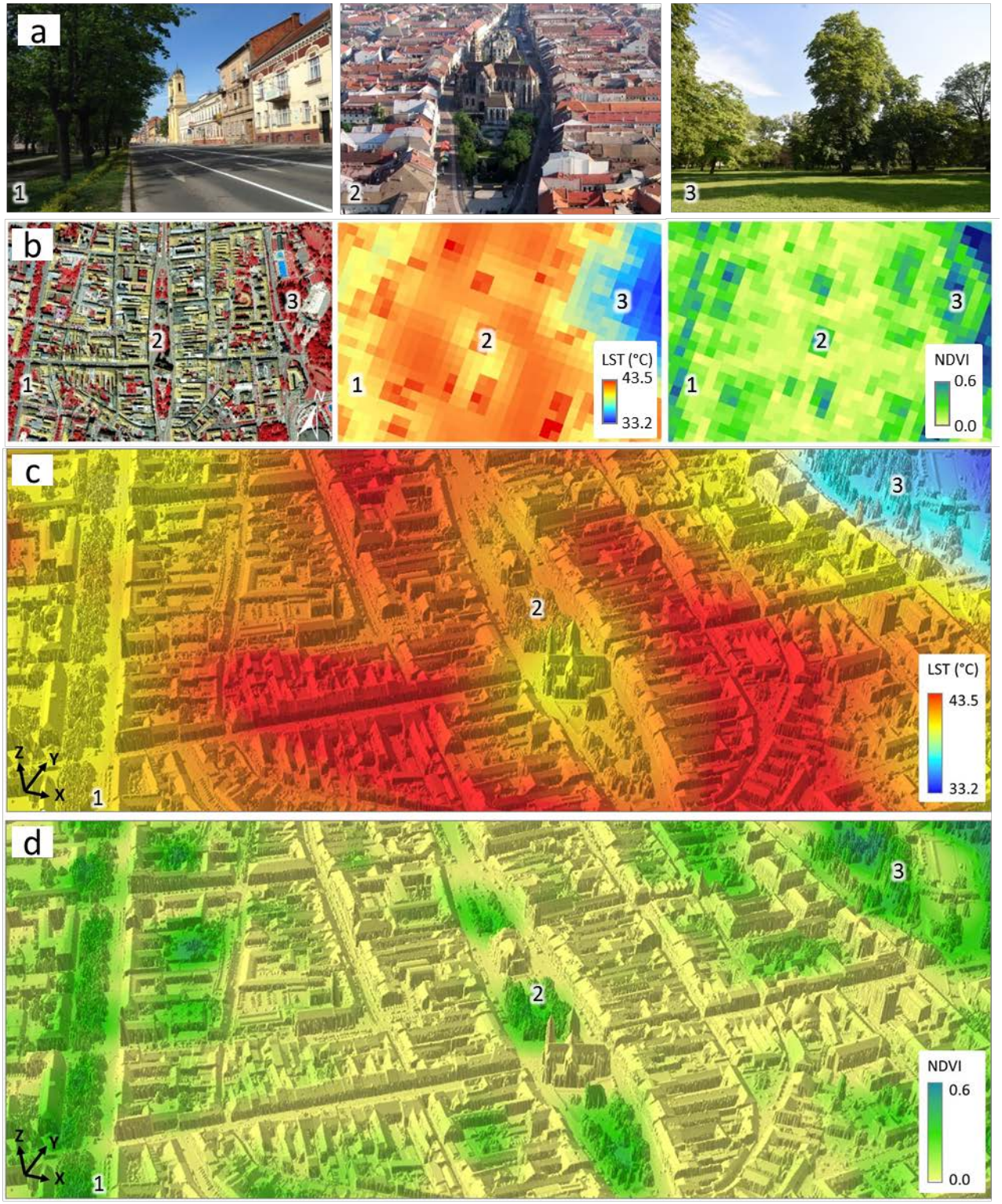

Figure 6. LST and NDVI values on 6 August 2015 in selected areas of the historical city centre of Košice (A): 1 – green alley on Moyzesova Street, 2 – the core of the city-centre, 3 – city park. (B) perspective 3D view of the LST model resampled to 0.5 m resolution draped over the lidar based digital surface model described in Hofierka et al., (2017).

The UHI was proved to exist in Košice using the coarser MODIS data by Schwarz et al., (2011) in their analysis of 263 European cities but more detailed spatial analysis of LST and the UHI phenomenon is provided in our study using the higher resolution data acquired by Landsat 7 and Landsat 8. Clear differences in average LST were found among individual CLC 2012 land cover categories which is in accordance with results for cities of similar size and land cover pattern such as Brno (Dobrovolný, 2013)

or Bratislava (Rusňák & Lieskovský, 2017). The calculated LST averages can be in our case affected into some extent by the difference in data currency between CLC valid to 2012 and the analyzed Landsat 8 image from 2015 but visual inspection of the imagery did not reveal larger land cover changes than the minimal mapping area of CLC 2012. The analysis of weather conditions in relation to LST exploited only three stations where the air temperature, relative air humidity and cloudiness were measured and available for the time of sensing the satellite scenes.

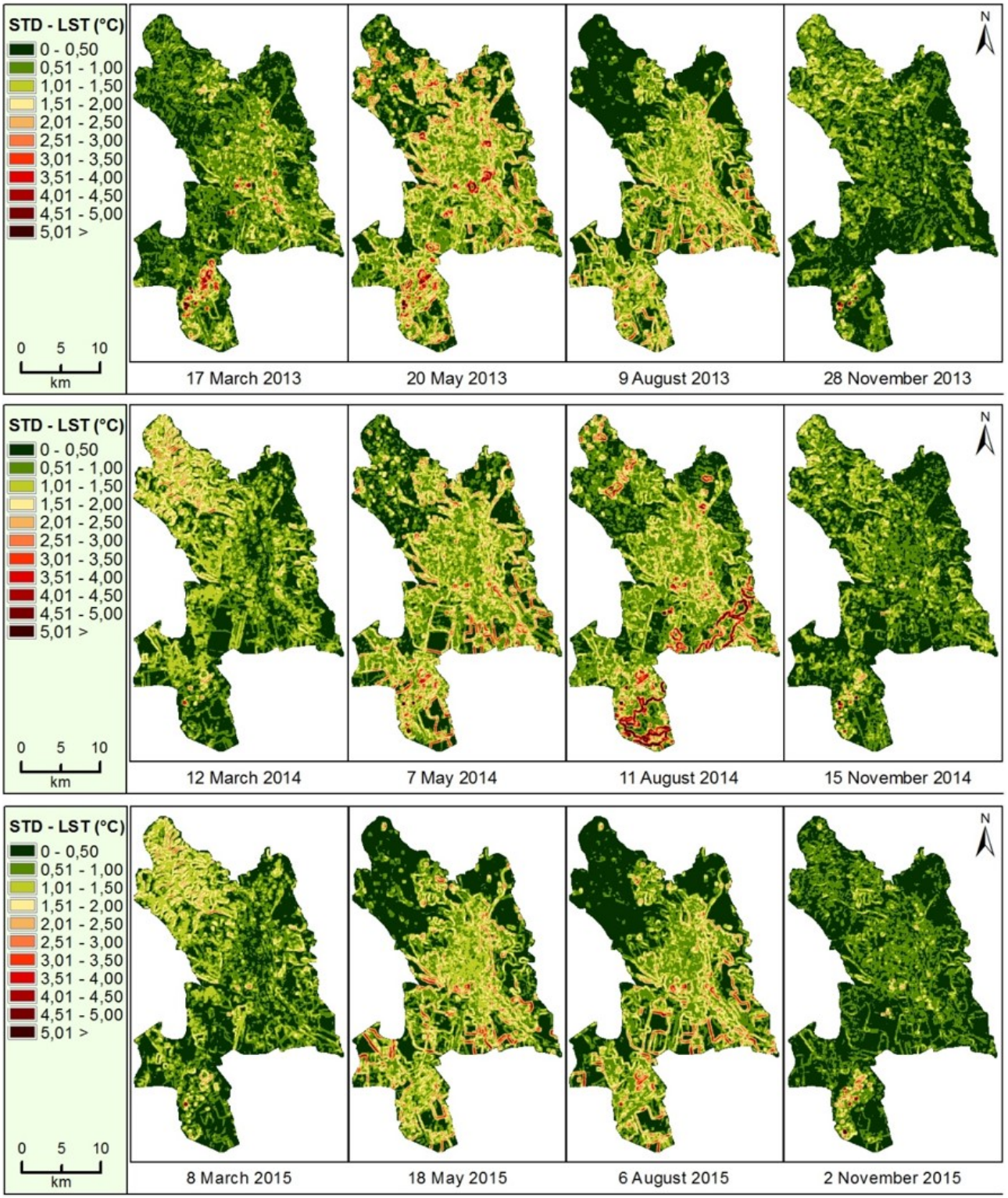

Figure 7. Spatial distribution of LST standard deviations for selected months in the period of 2013-2015 calculated from the LST raster layers as focal statistics in moving window of 7x7 cells for the study area of the Košice City.

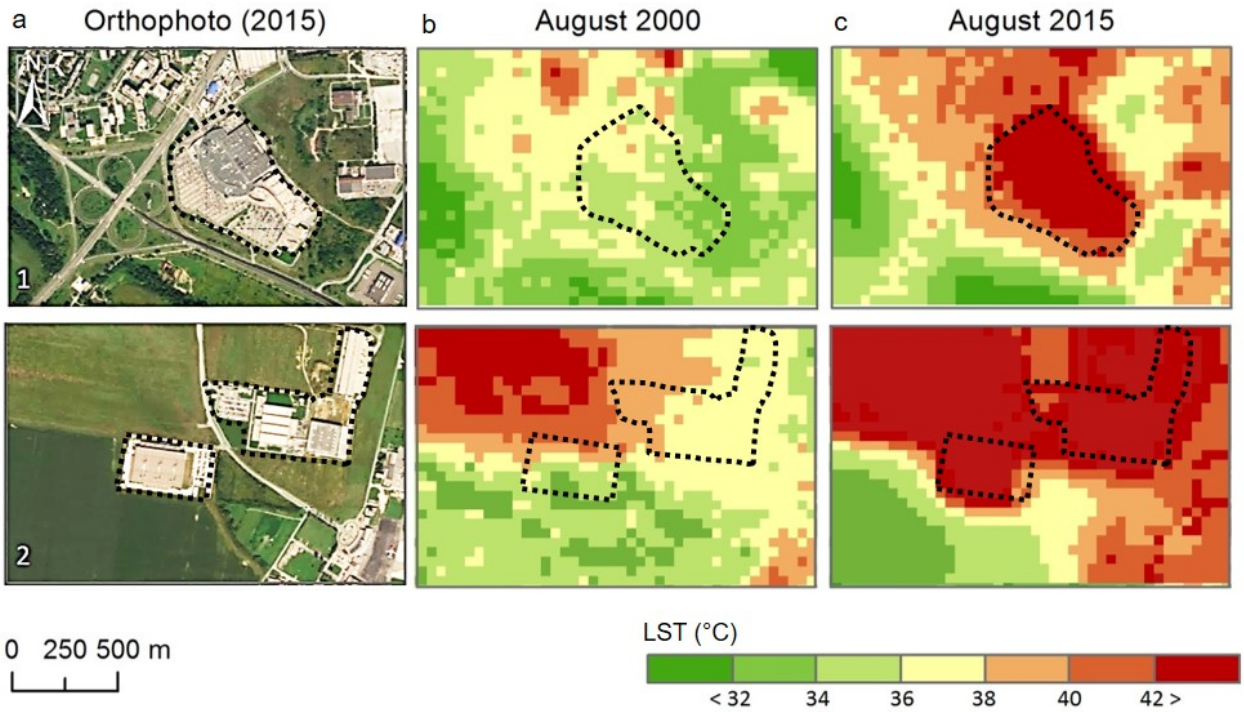

Figure 8. Comparison of LST in summer for areas in Košice where original semi-natural grassland and arable land was substituted with shopping centre (1) and industrial park (2). (a) Orthophotoimage of contemporary landscape (©ESRI, Basemap), (b) LST before construction on 8 August 2000, and after the change of land cover on 6 August 2015.

But still the defined linear regression models revealed similar relationships of similar strength and direction as by Giannaros et al., (2010) for Thessaloniki and by Kim & Baik (2004) for six large cities of South Korea. The linear regression model indicates that temperature of land surface in Košice tends to be more around 6°C higher than the air temperature measurement. Intermediate negative correlation was found between relative air humidity and LST. Assuming that green plants contribute to the higher air humidity, the finding indicates that LST can be mitigated by the presence of green vegetation within the city.

Finding a strong correlation between the NDVI and LST agrees with other studies such as Chen et al., (2015) for Beijing. This provides evidence that even in a small city green vegetation can mitigate UHI efficiently. However, this effect is strongest in the growing season while it is weak during the dormant season. Also smaller areas of vegetation and green belts located along roads and built-up areas were able to effectively reduce temperature. However, when comparing our results to those of other similar studies, it must be pointed out that some cities has already ingeniously designed systems that effectively ease the LSTs within the city, such as green wedges in Poznań (Majkowska et al., 2016). In Košice, there are few cases of similarly organized tree alleys of trees but more of such features in urban planning should be introduced in the future.

Temporal analysis of the LST local differences revealed, that the effect of UHI in the Košice city is the most pronounced during May and August. It can be explained by higher occurrence of days with the low cloud cover and mid-term of the growing season, when the urban greenery in the city is the most developed, therefore reduction of LST by the greenery is the strongest.

On the contrary, low local LST differences in March and November can be related to the dormant season. However, differences between the city and rural area can be significant also in winter, but the winter season was not subject to the conducted analysis in the presented research as from the health safety point of view the highest risk occurs in the summer.

6. CONCLUSION

The urban heat island (UHI) phenomenon concerns also small cities of several hundred thousands of inhabitants. Košice in Easter Slovakia is an example of such a city in mid-latitudes of Central Europe. Landsat 7 and Landsat 8 missions provide valuable multispectral imagery which we used to conduct spatio-temporal analysis of land surface temperature (LST) in Košice in recent years.

The results show that Košice experience higher LST in the built-up areas than in the surrounding landscape comprising forests or grassland which

provides evidence of the UHI phenomenon in the city. Given the analysed period between March and November, UHI is most pronounced in the summer.

Clear positive strong correlation was found between the air temperature and the LST based on the analysed LST datasets and three weather stations. LST was found to be in a strong negative correlation with NDVI in the growing season when plants have high chlorophyll content. Even small areas such as tree alleys or small gardens and parks with green vegetation within the urban fabric can mitigate the LST.

The results provided several examples that exchange of the semi-natural grassland or agricultural land for new shopping centres, commercial zones or industrial parks in the last two decades amplified the UHI effect and contributed to its expansion into suburban zones.

Elimination of the UHI effect and the effort for balanced presence of built-up areas and greenery in the further development of the city should be a priority for the upcoming years for the city management. Only in the harmony of these elements, the city can remain a full-valued environment for its inhabitants.

The future research of spatial aspects of LST in Košice or other cities could exploit the advance of new earth observation satellite missions, such as Sentinel 2. This mission provides higher spatial, temporal and spectral resolution in the near infrared spectral domain than the Landsat 8 data. Despite not having the thermal band, Sentinel 2 can provide higher resolution of NDVI for estimating the thermal emissivity of land cover for LST calculation from Landsat 8 TIRS thermal data.

Acknowledgements

This work originated within the feasibility study funded by the Government of Slovakia through an European Space Agency contract no. 4000117034 (SURGE) under the Plan for European Cooperating States (PECS). The view expressed herein can in no way be taken to reflect the official opinion of the European Space Agency. The research was also partially supported by the Ministry of Education, Science, Research and Sport of the Slovak Republic within the projects VEGA 1/0963/17 and VEGA 1/0474/16.

REFERENCES

Barsi, J. A., Schott J. R., Palluconi, F. D. & Hook, S. J., 2005. *Validation of a web-based atmospheric correction tool for single thermal band instruments.* Proceedings of SPIE, 5882, 136-142, http://dx.doi.org/10.1117/12.619990

Camilloni, I. & Barrucand, M., 2011. *Temporal variability of the Buenos Aires, Argentina, urban heat island.* Theoretical and Applied Climatology. 2012, 107 (1-2); doi:10.1007/s00704-011-0459-z

Chen, W., Zhang, Y., Gao, W. & Zhou, D., 2015. *The Investigation of Urbanization and Urban Heat Island in Beijing Based on Remote Sensing.* Procedia – Social and Behavioral Sciences, 216, 141-150.

Cheval, S. & Dumitrescu, A., 2009. *The July urban heat island of Bucharest as derived from Modis images.* Theoretical and Applied Climatology, 96 (1–2), 145-153, http://dx.doi.org/10.1007/s00704-008-0019-3.

Cheval, S., Dumitrescu, A. & Petrişor, A.-I., 2011. *The July Surface Temperature Lapse In The Romanian Carpathians.* Carpathian Journal of Earth and Environmental Sciences, 6 (1), 189-198.

Dobrovolný, P., 2013. *The surface urban heat island in the city of Brno (Czech Republic) derived from land surface temperatures and selected reasons for its spatial variability.* Theoretical and Applied Climatology, 112, 89-98, http://dx.doi.org/10.1007/s00704-012-0717-8.

Fabrizi, R., Bonafoni, S. & Biondi, R., 2010. *Satellite and Ground-Based Sensors for the Urban Heat Island Analysis in the City of Rome.* Remote Sensing, 2010, vol. 2, no. 5, 1400-1415, http://dx.doi.org/10.3390/rs2051400

Gerçek, D. Güven, İ.T. & Oktay, İ.Ç, 2016. *Analysis of the intra-city variation of urban heat island and its relation to land surface/cover parameters.* The International Archives of the Photogrammetry, Remote Sensing and Spatial Information Sciences (ISPRS Archives), VI, WG VI/4, pp. 123-129.

Giannaros, T. M., Melas, D. & Kontogianni, P., 2010. *An Observational Study of the Urban Heat Island in the Greater Thessaloniki Area: Preliminary Results and Development of a Forecasting Service.* AIP Conference Proceedings, vol. 1203 (1), 991-996.

Hofierka, J., Gallay, M., Kaňuk, J., Šupinský, J. & Šašak, J., 2017. *High-resolution urban greenery mapping for micro-climate modelling based on 3D city models.* The International Archives of the Photogrammetry, Remote Sensing and Spatial Information Sciences (ISPRS Archives), XLII-4/W7, pp. 7-12.

Kim, Y.-H. & Baik, J.-J., 2004. *Daily maximum urban heat island intensity in large cities of Korea.* Theoretical and Applied Climatology, 79 (3/4), 151-164.

Klok, L., Zwart, S., Verhagen, H. & Mauri, E., 2012. *The surface heat island of Rotterdam and its relationship with urban surface characteristics*. Resources, Conservation and Recycling, 64, 23-29

Li, Z.-L., Tang, B.-H., Wu, H., Ren, H., Yan, G., Wan, Z., Trigo, I. F. & Sobrino, J. A., 2013. *Satellite-derived land surface temperature: Current status and perspectives.* Remote Sensing of Environment, 131, 2013, 14-37.

Levermore, G., Parkinson, J., Lee, K., Laycock, P. & Lindley, S., 2017. *The increasing trend of the urban heat island intensity*. Urban Climate, https://doi.org/10.1016/j.uclim.2017.02.004.(Article in Press).

Lokoshchenko, M.A., 2014. *Urban 'heat island' in Moscow*. Urban Climate, 10, 2014, 550-562, http://dx.doi.org/10.1016/j.uclim.2014.01.008.

Loveland, T.R. & Irons, J.R., 2016. *Landsat 8: The plans, the reality, and the legacy*. Remote Sensing of Environment, 185, 2016, 1-6, http://dx.doi.org/10.1016/j.rse.2016.07.033.

Majkowska, A., Kolendowicz, L., Półrolniczak, M., Hauke & J., Czernecki, B., 2016: *The urban heat island in the city of Poznań as derived from Landsat 5 TM*. Theoretical and Applied Climatology, 64, 769-783.

Mucsi, L., Muladi, B., Henits, L., Farsang, A. & Albrect, V., 2014: *Large scale urban heat islands mapping based on spatial information provided by young volunteers.* Carpathian Journal of Earth and Environmental Sciences, 9 (2), 31-43.

NASA, 2013. *National Aeronautics and Space AdministrationProgram-level Requirements on the Landsat Data Continuity Mission Project: Appendix N to the Earth Systematic Mission Program Plan*, Washington, DC 20 p.

Oke, T. R., 1973. *City size and the urban heat island.* Atmospheric Environment, 7 (8), 769-779.

Pongrácz, R., Bartholy, J. & Dezső, Z., 2010. *Application of remotely sensed thermal information to urban climatology of Central European cities*, Physics and Chemistry of the Earth, Parts A/B/C, 35 (1), 95-99, http://dx.doi.org/10.1016/j.pce.2010.03.004.

Rajasekar, U. & Weng, Q., 2009**.** *Spatio-temporal modelling and analysis of urban heat islands by using Landsat TM and ETM+ imagery.* International Journal of Remote Sensing, 30 (13), 3531-3548.

Rusňák, T. & Lieskovský, J., 2017. *Calculation of Land Surface Temperature in Bratislava by Satellite Images.* Životné prostredie, 2017, 51(1), pp. 37 – 40.

Schwarz, N., Lautenbach, S. & Seppelt, R., 2011. *Exploring indicators for quantifying surface urban heat islands of European cities with MODIS land surface temperatures.* Remote Sensing of Environment, 115, (12), 2011, pp. 3175-3186.

Stathopoulou, M., Cartalis, C. & Keramitsoglou, I., 2004. *Mapping micro-urban heat islands using NOAA/AVHRR images and CORINE Land Cover: An application to coastal cities of Greece.* International Journal of Remote Sensing, 25 (12), pp. 2301-2316.

Švec, M., Faško, P., Labudová, L., Výberči, D. & Trizna, M. 2016. *Longterm Changes in the characteristics of heat stress in the summer in Slovakia.* Geographia Cassoviensis, 10 (2), pp. 193-203.

Voogt, J.A. & Oke, T.R., 2003. *Thermal remote sensing of urban climates*, Remote Sensing of Environment. 86 (3), 370-384.

Výberči, D., Labudová, L., Eštóková, M., Faško, P. & Trizna, M., 2017. *Human mortality impacts of the 2015 summer heat spells in Slovakia*. Theoretical and Applied Climatology, pp. 1-12. Article in Press. https://doi.org/10.1007/s00704-017-2224-4

Wulder, M.A., White, J.C., Loveland, T. R., Woodcock, C. E., Belward, A.S., Cohen, W.B., Fosnight, E. A., Shaw, J., Masek, J. G. & Roy, D.P., 2016. *The global Landsat archive: Status, consolidation, and direction*. Remote Sensing of Environment, 185, 271-283, http://dx.doi.org/10.1016/j.rse.2015.11.032.

Zhang, J., Wang, Y. & Li, Y., 2006. *A C++ program for retrieving land surface temperature from the data of Landsat TM/ETM+ band 6.* Computers and Geosciences, 32 (10), 1796-1805.

Received at: 12. 11. 2017
Revised at: 10. 01. 2018
Accepted for publication at: 16. 01. 2018
Published online at: 23. 01. 2018